Journal of Hydroscience and Hydraulic Engineering
Vol. 18, No.2 November, 2000, 63-74

UNSTEADINESS EFFECTS ON INNER-LAYER CHARACTERISTICS IN SMOOTH OPEN-CHANNEL FLOWS

By

Kouki Onitsuka
Research Associate, Department of Civil and Global Environment Engineering
Kyoto University, Kyoto 606-8501, Japan

and

Iehisa Nezu
Professor, Department of Civil and Global Environment Engineering
Kyoto University, Kyoto 606-8501, Japan

SYNOPSIS

The inner region including the viscous sublayer in unsteady smooth open channel flows with strong unsteadiness was measured accurately by making use of an innovative two-component laser Doppler anemometer(LDA). The von Karman constant κ was evaluated by making use of the friction velocity which was calculated from a linear formula in the viscous sublayer. The von Karman constant decreases slightly in the rising stage and increases in the falling stage in comparison with the value of steady uniform open-channel flows(κ =0.41). The turbulence intensity distributions in the buffer layer can be described well by a van Driest's damping function, in which the van Driest's damping factors are almost constant irrespective of the unsteadiness. The third order moments of turbulence agree well with those of steady uniform channel flows.

INTRODUCTION

One of the most dangerous natural disasters is flood flows. If the land is flooded, a great deal of damage occurs. Rivers in flood are characterized by unsteadiness of the flow. It is necessary to investigate hydrodynamic characteristics in unsteady open-channel flows. Many researchers have observed and measured these flooded flows in rivers. It was often observed that a peak discharge appears before a time of peak depth and the concentration of suspended sediment in the rising stage is larger than that in the falling stage.

Open-channel flows consist of an inner region and an outer region. Further, the inner region consists of the viscous sublayer, buffer layer and log layer. Turbulence measurements not only in the outer layer but also in the inner layer have been conducted in the case of uniform open-channel flows. The characteristics of the inner region in steady open channel flows were investigated completely by Nezu & Rodi(1986) and Onitsuka & Nezu(1998) by making use of a laser Doppler anemometer(LDA). They found that the von Karman constant and the integral constant are universal ones, irrespective of the Reynolds and Froude numbers and also that the friction velocities evaluated from both the linear formula in the viscous sublayer and the log-law were in a good agreement with each other.

In contrast, turbulence measurements of only the outer region were conducted in the case of unsteady open-channel flows. Hayashi *et al.*(1988) have suggested that the turbulence in the outer region becomes stronger in the rising stage than in the falling stage by making use of a hot-film anemometer. Tu & Graf (1992) and Song & Graf(1996) have measured unsteady open channel flows over gravel beds by making use of a micro-propeller flow-meter and an acoustic Doppler velocity profiler, respectively. They have examined the unsteadiness effects on turbulent structures by making use of Clauser's equilibrium pressure gradient parameter and pointed out that the Reynolds stress distributions can be predicted semi-theoretically under the assumption that the mean velocity distributions are expressed by a power law and the flows are

in equilibrium. Nezu & Nakagawa(1991) have measured unsteady smooth and rough open-channel flows by making use of a two component laser Doppler anemometer(LDA) with high accuracy, and have indicated that a peak discharge appears before a time of peak depth in proportion to the unsteadiness. Further more, they pointed out that mean velocity distributions up to the free surface can be described by the log-law in the case of low Reynolds numbers and also can be described by the log-wake law in the case of high Reynolds numbers.

Until recently, turbulence measurements in the viscous sublayer have been almost impossible by making use of conventional velocimetries such as pitot tube, propeller flow meter, electromagnetic flow meter, hot-film anemometer and acoustic Doppler verlocimetry(ADV). This is because a thickness of the viscous sublayer is much smaller than the sensor scales of these anemometers. Nezu, Kadota & Nakagawa (1997) firstly measured the viscous sublayer successfully in unsteady depth-varying open-channel flows which have a hydrograph of sine curve, and they have pointed out that the von Karman constant is an almost universal constant although it may change slightly and complicatedly against the duration time. However, their experimental conditions for measurements of viscous sublayer include only one unsteadiness case for both monotonically increasing and decreasing flows.

In the present study, turbulence measurements of unsteady open-channel flows including the stronger unsteadiness were conducted by making use of an innovative two-component laser Doppler anemometer(LDA). The effects of unsteadiness upon the von Karman constant and the integration constant of the log law were investigated intensively. Further more, the third-order moments of the turbulence were firstly investigated with high accuracy.

THEORETICAL CONSIDERATIONS

The shear stress distribution of 2-D steady open-channel flows can be obtained from the equation of motion, as follows:

$$\frac{\tau}{\rho U_*^2} \equiv \frac{-\overline{uv}}{U_*^2} + \frac{dU^+}{dy^+} = 1 - \frac{y^+}{R_*} \tag{1}$$

in which, U is the mean velocity component in the streamwise direction, x, U_* is the friction velocity, $-\overline{uv}$ is the Reynolds stress and τ is the total shear stress. $U^+ \equiv U/U_*$, $R_* \equiv hU_*/\nu$ and $y^+ \equiv yU_*/\nu$ is the vertical coordinate normalized by the inner variables, in which y is the vertical coordinate and ν is the kinematic viscosity. Eliminating the Reynolds stress with the aid of Prandtl's mixing length model, Eq.(1) reads:

$$\frac{dU^+}{dy^+} = \frac{2(1-\xi)}{1+\sqrt{1+4\ell^{+2}(1-\xi)}} \tag{2}$$

in which, $\xi \equiv y/h$ is the coordinate normalized by the outer variables, $\ell^+ \equiv \ell U_*/\nu$ is the mixing length normalized by inner variables. In the near wall-region, the linear mixing length is modified by the van Driest's damping function Γ, as follows:

$$\ell^+ = \kappa y^+ \Gamma \tag{3}$$

$$\Gamma = 1 - \exp\left(-\frac{y^+}{B}\right) \tag{4}$$

in which, κ is the von Karman constant and B is the damping factor. In the viscous sublayer ($0 < y^+ \leq 5$), Eq.(2) can be reduced to:

$$U^+ = y^+ \tag{5}$$

In the log layer ($B < y^+$), Eq.(2) can be reduced to:

$$U^+ = \frac{1}{\kappa}\ln y^+ + A \tag{6}$$

The normalized turbulence intensities u'/U_* and v'/U_* are described by Nezu's empirical formulae, as follows (see Nezu & Nakagawa, 1993):

$$\frac{u'}{U_*} = D_u \exp(-\lambda_u \xi) \tag{7}$$

$$\frac{v'}{U_*} = D_v \exp(-\lambda_v \xi) \tag{8}$$

in which, D_u =2.26, D_v =1.23, λ_u =0.88 and λ_v =0.67 are empirical constants which were obtained by Nezu &

Rodi(1986) in 2-D open-channel flows with LDA system. In the buffer layer ($5 < y^+ < B$), Eqs.(7) and (8) are modified due to the viscous effects, in the followings:

$$\frac{u'}{U_*} = D_u \exp\left(-\lambda_u \frac{y^+}{R_*}\right)\Gamma + Cy^+(1-\Gamma) \tag{9}$$

$$\Gamma = 1 - \exp\left(-\frac{y^+}{B_{ut}}\right) \tag{10}$$

in which, C is the empirical coefficient. In the viscous sublayer, Eq.(9) can be reduced to:

$$\frac{u'}{U_*} = Cy^+ \tag{11}$$

Nezu & Rodi(1986) found experimentally that C is constant value(≈ 0.3) in 2-D open-channel flows, irrespective of the Reynolds and Froude numbers.

EXPERIMENTAL EQUIPMENT AND DATA PROCESSING

The present experiments were conducted in a 10-m-long, 40-cm-wide, and 50-cm-deep tilting flume. In this water flume, the discharge Q can be automatically controlled by a personal computer in which the rotation speed of a water-pomp motor involving an inverter transistor is controlled by the feedback from the signals of an electromagnetic flow meter.

Two components of instantaneous velocities, i.e., the streamwise velocity $\tilde{u}(t)$ and the vertical velocity $\tilde{v}(t)$, were measured with a four-beam fiber-optic LDA system (DANTEC-made). The present LDA system can measure instantaneous velocities very near the wall. The LDA was located 8m downstream of the channel entrance so that, the turbulent flow was fully developed. The water-wave gauge was located 10cm downstream of the velocity measuring points. The LDA fiber probe was moved by three-dimensional traversing mechanism. The accuracy of this traversing mechanism was within 1/100mm. The measurements very near the wall, i.e., up to y =0.1mm, were successfully conducted accurately. All of output signals of the LDA and water-wave gauge were recorded in a digital form with a sampling frequency more than f =100(Hz) into a HDD of the personal computer. After experiments, all of the experimental data were transferred to the workstation through the LAN.

It is very important for investigation of unsteady flow to determine the time-dependent mean velocity component $U(t)$ from the instantaneous velocity component $\tilde{u}(t) = U(t) + u(t)$. In general, there are three kind of methods, as followings:

a) Ensemble-average method, b) Moving time-average method, c) Fourier-component method.

Method a) is often used in the investigations on oscillatory pipe flows, closed-channel flows, and unsteady boundary layers. Nezu & Nakagawa(1991) and Song & Graf(1996) pointed out that the method c) is the most reasonable for unsteady open channel flows. In this study, the method c) was, therefore, adopted. The Fourier component m was adopted as seven, which were used by Nezu & Nakagawa(1991). More detailed information is available in Nezu, Kadota & Nakagawa(1997). Experimental conditions are shown in Table 1. In which, U_m is the bulk mean velocity, $Re \equiv U_m h/\nu$ is the Reynolds number based on the bulk mean velocity U_m, $R_* \equiv U_* h/\nu$ is the Reynolds number based on the friction velocity and $Fr \equiv U_m/\sqrt{gh}$ is the Froude number. T_d is the duration time from the base discharge to the peak discharge in flood. The suffix b means the value before the flood, i.e, in "base" flow and suffix p means the value at the "peak" depth. α is the unsteadiness parameter proposed by Nezu & Nakagawa(1991), as follows:

$$\alpha = \frac{2}{U_{mb} + U_{mp}} \frac{h_p - h_b}{T_d} \tag{12}$$

Table 1 Hydraulic Conditions

Case Name	α $\times 10^{-3}$	T_d (s)	h_b (cm)	h_p (cm)	U_{mb} (cm/s)	U_{mp} (cm/s)	R_{*b}	R_{*b}	R_{eb} $\times 10^3$	R_{ep} $\times 10^4$	Fr_b	Fr_p
U3	3.01	60	6.0	7.5	3.33	13.3	154	494	2.24	1.12	0.04	0.16
U2	1.86	120		7.8		12.8	156	587	2.32	1.16	0.04	0.15
S3	2.94	60	7.2	8.5	4.17	10.6	216	434	3.00	0.90	0.05	0.12

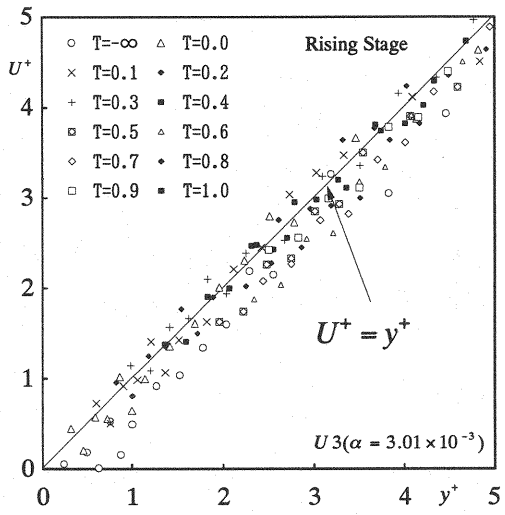

Fig.1(a) Velocity distribution of viscous sublayer in rising stage

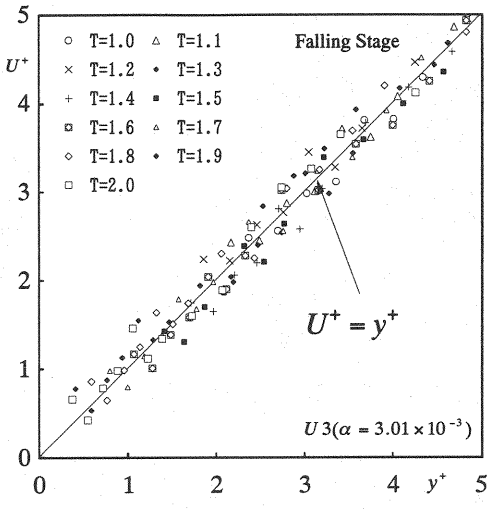

Fig.1(b) Velocity distribution of viscous sublayer in falling stage

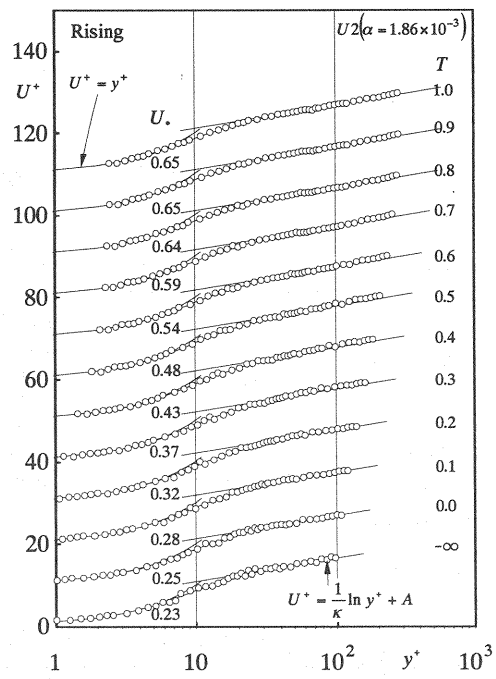

Fig.2(a) Velocity distributions in rising stage, i.e. T<1

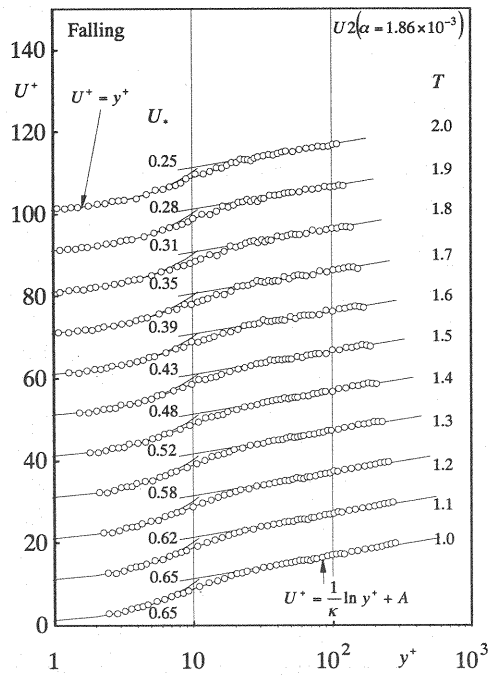

Fig.2(b) Velocity distributions in falling stage, i.e. T>1

RESULTS AND DISCUSSIONS

Evaluation of Friction Velocity and von Karman Constant κ

Fig.1 shows the mean velocity distributions in the viscous sublayer($0< y^+ \leq 5$) in the rising stage and falling stage. The symbol of the time before the increase of the water depth is denoted as $-\infty$. The mean velocity distributions in the viscous sublayer fit well to the linear formula of (5), which is derived analytically from the equation of motion. The friction velocity U_* was evaluated from the linear formula of (5).

Fig.2 shows the mean velocity distributions in the inner and outer regions in the case of S3. Over the buffer layer ($30 \leq y^+$), the velocity distributions are described by the log-law, which is shown by the straight lines in Fig.2, up to the free surface. Nezu & Rodi(1986) indicated that the log-law is valid up to the free surface in the range of low Reynolds numbers in which R_* attains up to 500 in the case of steady open-channel flows. The log-wake law is, however, necessary at high Reynolds numbers in which R_* is greater than 500, as have pointed out by Nezu & Rodi(1986). This Nezu & Rodi's criterion seems to be valid even in unsteady open-channel flows.

The von Karman constant κ can be calculated from the log-law of (6), by making use of the friction velocity U_{*1} which was evaluated from the linear formula of (5). Fig.3 shows the variations of the von Karman constant κ against the normalized time $T \equiv t/T_d$. Nezu, Kadota & Nakagawa's (1997) data, which were obtained in monotonically rising and falling flows, were also plotted in Fig.3 by black symbols. It was found that the values of κ increase suddenly near the initial time and decrease before the time of the peak depth. Next, the values of κ increase then with the normalized time and decrease before the end of the flood time. This tendency agrees with Nezu, Kadota & Nakagawa's (1997) results which were obtained in monotonically rising and falling flows. The deviation of von Karman constant κ from the steady value(κ =0.41) increases in

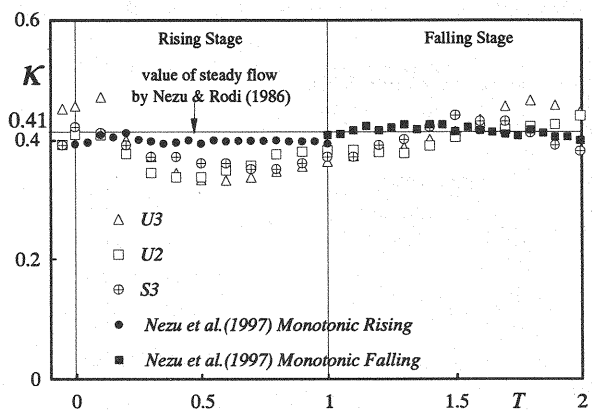

Fig.3 Variation of von Karman constant

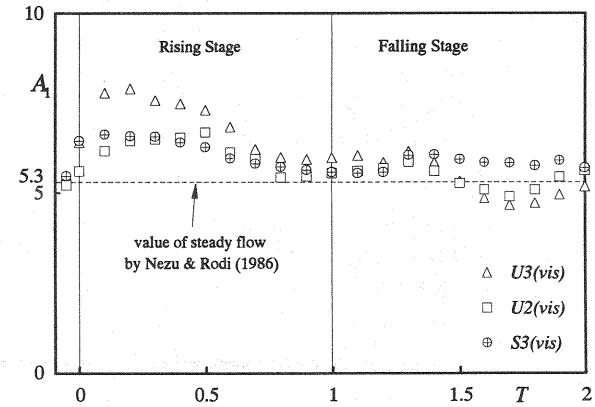

Fig.4 Integration constant A_1 against normalized time

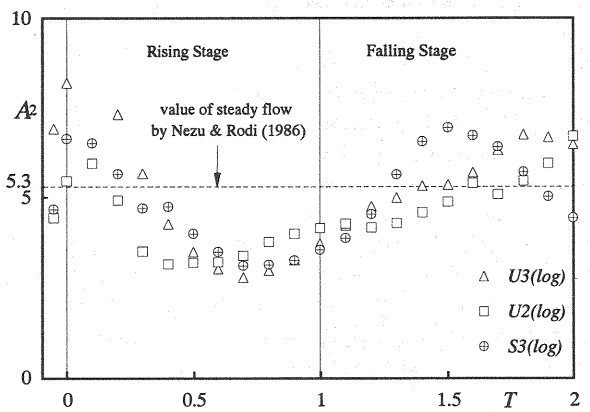

Fig.5 Integration constant A_2 against normalized time

proportion to the unsteadiness parameter α . Spalart & Leonald(1987) have calculated velocity profiles in turbulent boundary layers with pressure gradients by making use of a direct numerical simulation(DNS) and have shown that von Karman constant κ is not universal constant in the case of non-uniform flows. Therefore, the von Karman constant is affected by the pressure gradients, which is proportional to the unsteadiness parameter α .

Integration Constant A

The integration constant A_1 in the log law can be obtained by making use of the friction velocity U_{*1} which is evaluated from the linear formula of (5), i.e., the Method 1. Fig.4 shows the behavior of integration constant A_1 against the normalized time T . The integration constant A_1 increases in the rising stage and decreases in the falling stage.

In contrast, almost researchers have estimated the integral constant by making use of the friction velocity which is calculated from the log law of (6) under the assumption that the von Karman constant is an universal constant, i.e., κ =0.41, irrespective the unsteadiness, which is called here as the Method 2. However, the von Karman constant is influenced by strong unsteadiness. It is necessary to compare the results by Method 1 with those by Method 2. Fig.5 shows the behavior of integration constant A_2 against the normalized time. The value of A_2 decreases with normalized time and attains a minimum value before the time of peak depth, i.e., T <1. Its value increases then and attains a maximum value in the middle of the falling stage. This is because the unsteady flows are affected by the pressure gradient, as pointed out by Song & Graf (1996) and Nezu, Kadota & Nakagawa(1997).

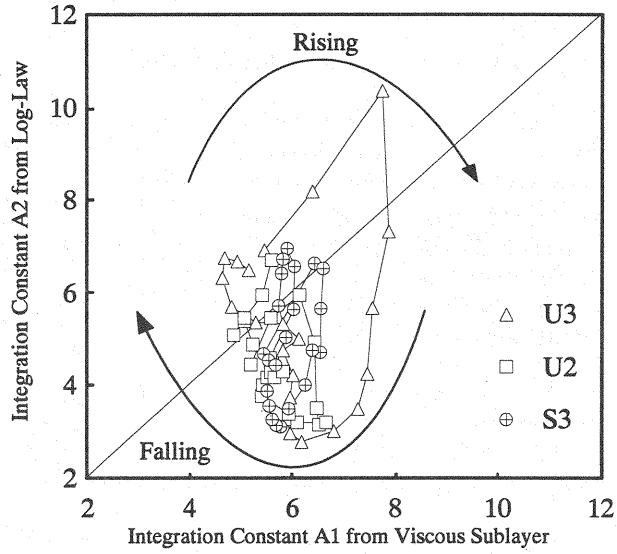

Fig.6 Relationship between A_1 and A_2

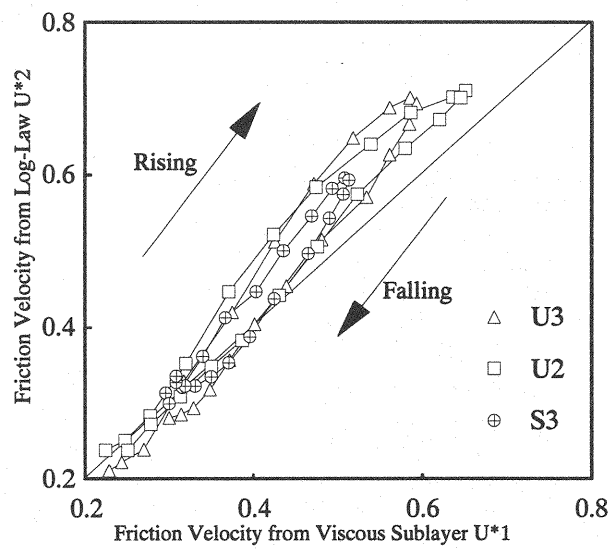

Fig.7 Relationship between U_{*1} and U_{*2}

Fig.6 shows the relationship between the integral constant A_1 and the integration constant A_2 . Both values do not coincide with each other and show a loop relationship. The circulation area increases with an increase of the unsteadiness. It is further necessary to investigate the unsteadiness effects on velocity profiles of open-channel flows in the wide range of weak and strong unsteadiness parameters.

Friction Velocity U_*

It is very important to evaluate the friction velocity accurately not only for normalized turbulence statistics but also for suspended sediment in river environment. This is because it is necessary to evaluate the friction velocity with high accuracy for predicting the bed-load transport rate and the concentration of the suspended sediment in flooded rivers. Fig.7 shows the relationship between the friction velocities(as U_{*1}) calculated by the linear formula of (5) and friction velocities (as U_{*2}) calculated by the log law of (6) under the assumption that the von Karman constant is same as the steady value(=0.41). The friction velocities U_{*2} deviate from the friction velocities U_{*1} with an increase of the normalized time in the rising stage. In the falling stage, this deviation decreases against the normalized time. These deviations tend to increase in proportion to the value of unsteadiness parameter α. The values of unsteadiness parameter α in this experiments are quite high(α =(1.9-3.0) $\times 10^{-3}$) in comparison with those of natural flood flows(α is almost less than 10^{-4}). Therefore, the friction velocity can be estimated even by the log law with high accuracy in natural flood flows.

Of course, the friction velocities U_{*1} are more accurate than U_{*2} in the case of the present laboratory smooth bed unsteadiness. Therefore, the values of U_{*1} is adopted the friction velocity U_* in the following.

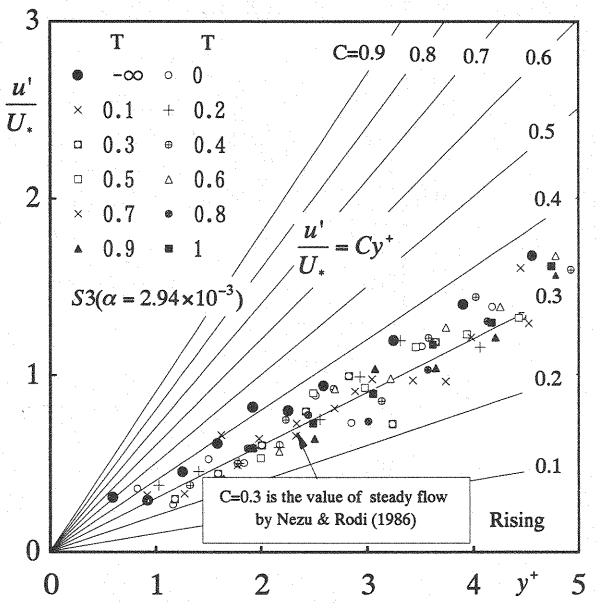

Fig.8(a) Distributions of turbulence intensity of viscous sublayer in rising stage

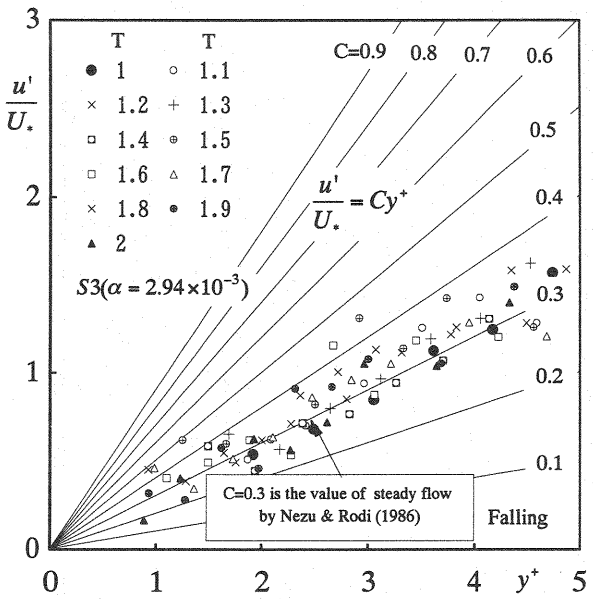

Fig.8(b) Distributions of turbulence intensity of viscous sublayer in falling stage

Turbulence Intensity

Fig.8 shows the distributions of the turbulence intensity $u' \equiv \sqrt{\overline{u^2(t)}}$ in the viscous sublayer normalized by the friction velocity U_* at the corresponding phase time. The normalized turbulence intensity u'/U_* can be described by a linear function, i.e. Eq.(11). The coefficient C can be determined from (11) by making use of the least-square method. Fig.9 shows the behavior of the coefficient C against the normalized time. Although there is

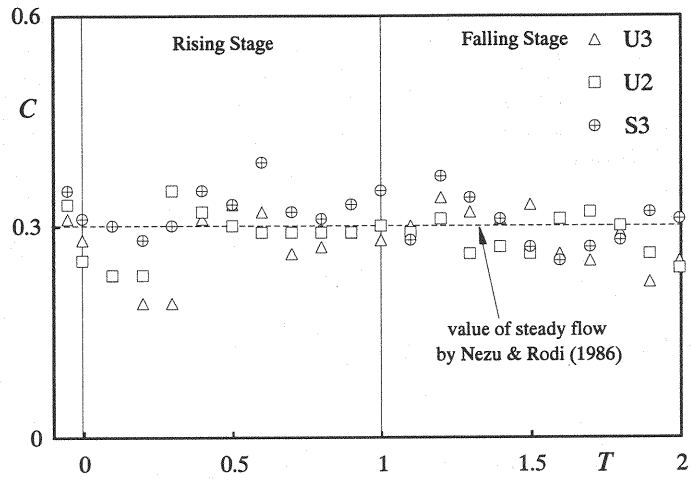

Fig.9 Variations of coefficient C against normalized time

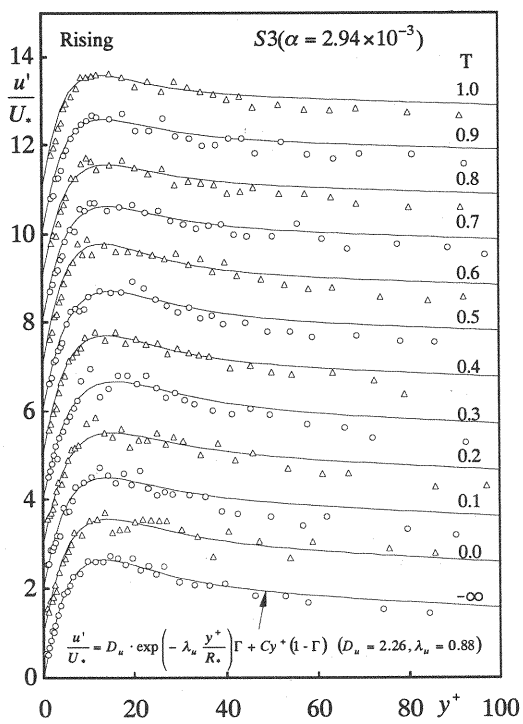

Fig.10(a) Distributions of turbulence intensity in rising stage

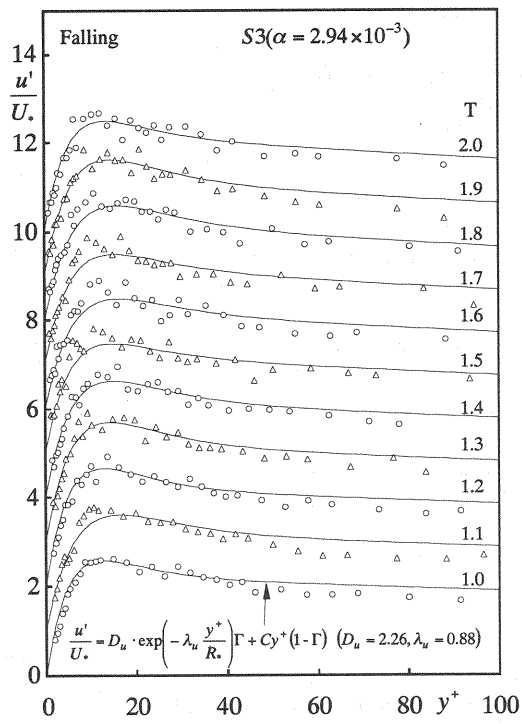

Fig.10(b) Distributions of turbulence intensity in falling stage

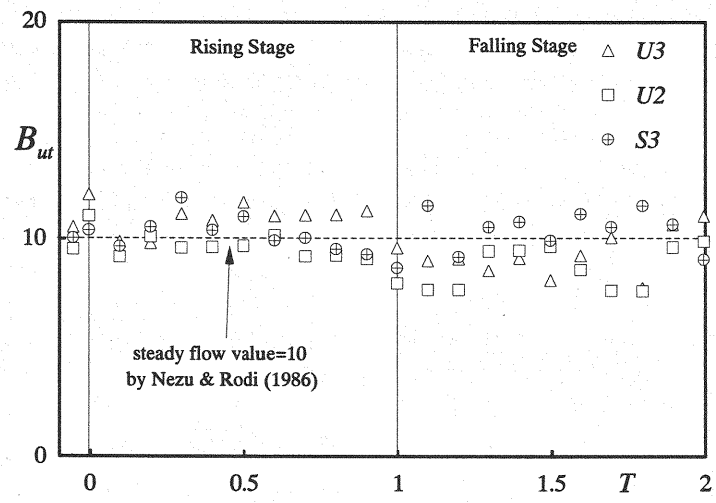

Fig.11 Variation of coefficient B_{ut} against normalized time

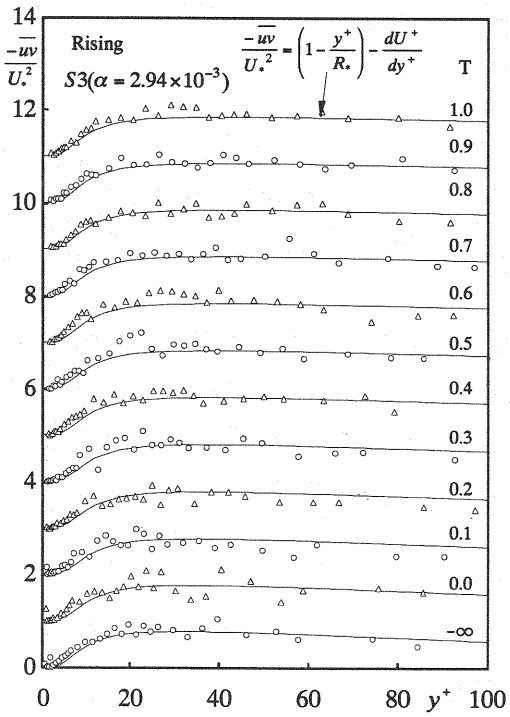

Fig.12(a) Distributions of Reynolds stress in rising stage

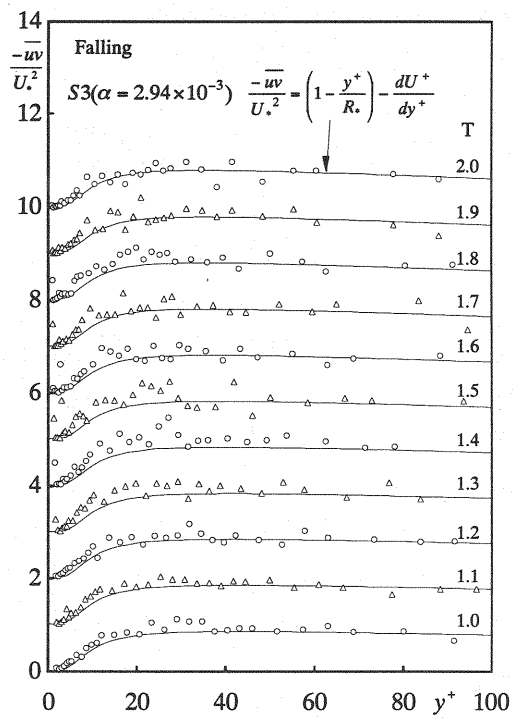

Fig.12(b) Distributions of Reynolds stress in falling stage

some scatter in data, no systematic deviation against the normalized time is seen. Therefore, the coefficient C is not affected by the unsteadiness so much at least when the range of the unsteadiness parameter α is less than 3.0×10^{-3}. This fact may be surprised compared with the characteristics of von Karman constant.

In the case of steady open-channel flow, Nezu & Rodi(1986) and Onitsuka & Nezu(1998) have found that the damping factor B_{ut} in Eqs.(9) and (10) is almost constant(≈ 10), irrespective of the Reynolds numbers and Froude numbers. In contrast, the damping factor B_{ut} in unsteady open channel flows has been unknown as yet. Fig.10 shows the distributions of the turbulence intensity u'/U_* in the wall region normalized by the friction velocity. The damping factor B_{ut} was determined with the least-square method so that the data in the region of $5< y^+ \leq 40$ gave the best fit to Eqs.(9) and (10). The calculated values of the turbulence intensity from Eqs.(9) and (10) are also included in Fig.10 by curved lines. The calculated curves coincide well with the measured data. The turbulence intensity attains a maximum value at $y^+ \approx 17$, which is in good agreement with steady open-channel flows investigated by Nezu & Rodi(1986). Fig.11 shows the behavior of the damping factor B_{ut} against the normalized time T. It can be seen that the damping factor B_{ut} is almost constant against the normalized time in all cases.

Reynolds stress Distributions $-\overline{uv}$

Fig.12 shows the distributions of the Reynolds stress $-\overline{uv}$ normalized by the friction velocity at the corresponding phase time, together with the theoretical curves of Eq.(1). Although Eq.(1) is not valid exactly in unsteady open-channel flows but valid only in steady open-channel flows, the experimental data in this study agrees well with Eq.(1) in almost regions. These facts suggest that the Reynolds shear stress distributions normalized by the corresponding friction velocity are not so much affected by the unsteadiness.

Third-order Moments of Turbulence

Until now, the third-order moments of the turbulence in unsteady open-channel flows have not been investigated at all in spite of these importance. These third-order moments are very important statistics because they relate with the bursting phenomena, as pointed out by Nakagawa & Nezu(1977) and because the third moments $\overline{uuv}$ and $\overline{vvv}$ constitute the diffusion term in a turbulent energy equation. Figs.13 and 14 show an example of distributions of $\overline{uuv}$ and $\overline{vvv}$ normalized by the friction velocity, together with Kim, Moin & Moiser's.(1987) DNS (Direct Numerical Simulation) data

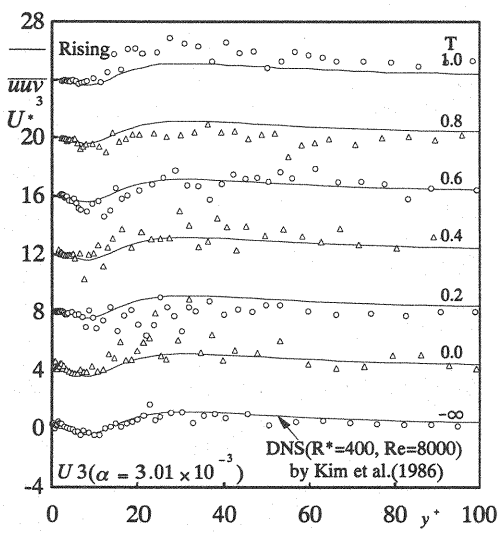

Fig.13(a) Distributions of $\overline{uuv}$ in rising stage

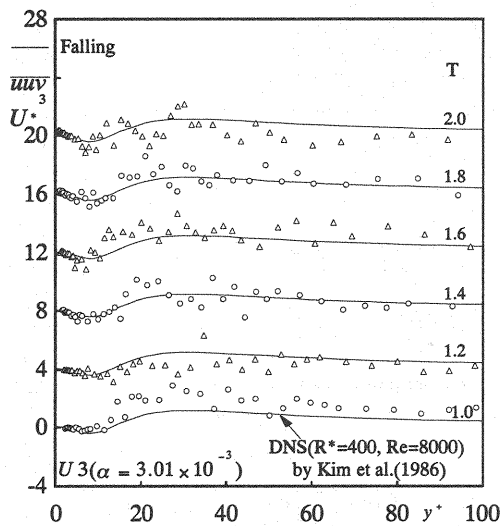

Fig.13(b) Distributions of $\overline{uuv}$ in falling stage

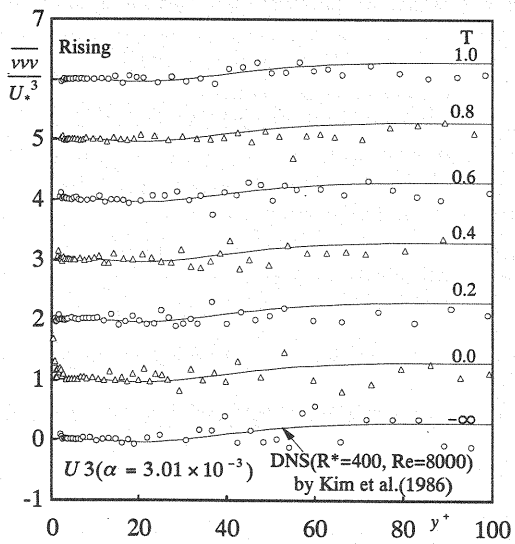

Fig.14(a) Distributions of $\overline{vvv}$ in rising stage

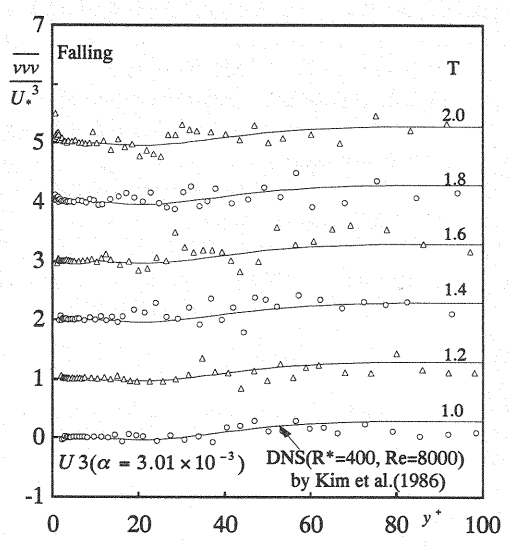

Fig.14(b) Distributions of $\overline{vvv}$ in falling stage

the diffusion term in a turbulent energy equation. Figs.13 and 14 show an example of distributions of $\overline{uuv}$ and $\overline{vvv}$ normalized by the friction velocity, together with Kim, Moin & Moiser's.(1987) DNS (Direct Numerical Simulation) data in a closed-channel flow at the Reynolds number $R_* = 400$ and $R_e = 8000$. Although there is some scatter in data, no systematic deviation can be seen. The present data agree well with DNS database. Therefore, it can be said that the third-order moments of turbulence are not affected by the unsteadiness.

CONCLUSIONS

Turbulence measurements in unsteady open-channel flows over a smooth bed at strong unsteadiness were conducted accurately with an LDA system.

The von Karman constant κ decreases slightly in the rising stage and increases in the falling stage in comparison with steady value(=0.41). Consequently, the friction velocity calculated by the log-law deviates slightly from that calculated by the linear formula in the viscous sublayer. In contrast, the coefficient C and the damping factor B_{ut} in the turbulence intensity are not so affected by the unsteadiness. The Reynolds stress and the third-order moments of the turbulence are also not so much affected by the unsteadiness.

REFERENCES

1. Hayashi, T., Ohashi, M. and Oshima, M.: Unsteadiness and turbulence structure of a flood wave, *Proc. of 20th Symp. on Turbulence,* pp.154-159, 1988 (in Japanese).
2. Kim, J., Moin, P. and Moser, R.: Turbulence statistics in fully developed channel flow at low Reynolds number, *J. Fluid Mech.*, vol.177, pp.133-166, 1987.
3. Nakagawa, H. and Nezu, I.: Prediction of the contributions to the Reynolds stress from the bursting events in open-channel flows, *J. Fluid Mech.*, vol.80, pp.99-128, 1977.
4. Nezu, I. and Rodi, W.: Open-channel flow measurements with a laser Doppler anemometer, *J. of Hydraulic Eng.*, ASCE, Vol.112, No.5, pp.335-355, 1986.
5. Nezu, I. and Nakagawa, H.: Turbulent structures over dunes and its role on suspended sediments in steady and unsteady open-channel flows, *Proc. of Int. Symp. on Transport of Suspended Sediments and its Mathematical Modeling*,

IAHR, Firenze, pp.165-189, 1991.
6. Nezu, I. and Nakagawa, H.: *Turbulence in Open-Channel Flows*, IAHR-Monograph, Balkema, Netherlands, 1993.
7. Nezu, I., Kadota, A. and Nakagawa, H. : Turbulent structure in unsteady depth-varying open-channel Flows, *J. of Hydraulic Eng.*, ASCE, Vol.123, No.9, pp.752-763, 1997.
8. Onitsuka, K. and Nezu, I.: Turbulent structure in the near-wall region of 2-D open channel flows, *Proc. of 7th Inter. Sympo. on Flow Modeling and Turbulence Measurements*, Tainan, Taiwan, pp.679-704, 1998.
9. Spalart, P.R. and Leonald, A.: Direct numerical simulation of equilibrium turbulent boundary layers, *Turbulent Shear Flows 5*, Springer-Verlag, Heidelberg, pp.234-252, 1987.
10. Song, T. and Graf, W.H.: Velocity and turbulence distribution in unsteady open-channel flows, *J. of Hydraulic Eng.*, ASCE, Vol.122, No.3, pp.141-154, 1996.
11. Tu, H. and Graf, W.H.: Velocity distribution in unsteady open-channel flow over gravel beds, *J. of Hydroscience and Hydraulic Eng.*, JSCE, Vol.10, pp.11-25, 1992.

(Received November 26, 1999 ; revised June 9, 2000)